Theory of the effect of supercurrents on the low-voltage resistance of superconductor–insulator–normal-metal tunnel junctions

Thomas R. Lemberger, Yeouchung Yen, and Soon-Gul Lee
Department of Physics, Ohio State University, Columbus, Ohio 43210
(Received 14 October 1986)

The theory of charge imbalance in tunnel junctions is adapted to describe the low-voltage resistance $R_j(T)$ of low-resistance superconductor–insulator–normal-metal (SIN) tunnel junctions. R_j is shown to be very sensitive to the pair-breaking effect of supercurrents. Numerical calculations for hypothetical SIN junctions illustrate how one can obtain information about the magnitude and temperature dependence of electron scattering rates, coherence factors, and the density of superconducting electrons from measurements of R_j in the presence of supercurrents either applied directly with a current supply or induced with a magnetic field applied parallel to the superconducting film. Such measurements should yield information similar to that obtained from other nonequilibrium techniques like NMR and ultrasonic attenuation.

I. INTRODUCTION

A great deal of work, both theoretical[1–13] and experimental,[14–24] has focused on charge-imbalance phenomena in tunnel junctions involving superconducting films. Experimental results near the superconducting transition temperature have been generally in good agreement with theoretical expectations. Data at lower temperatures often differ from theory. Despite the discrepancies, it is clear that in addition to their intrinsic interest, charge-imbalance phenomena offer the possibility to measure quantities such as the electron-phonon scattering rate, quantities that are difficult to measure in other ways. This possibility is the motivation for further work.

Several experimental studies[14–19] have dealt with a three-film, two-junction geometry in which the superconducting film to be studied is sandwiched between two other films. One junction is biased at a relatively high voltage to generate a charge imbalance in the superconducting film. The other junction detects the imbalance. This geometry has the favorable feature that the charge imbalance is generated with one junction and detected with another. However, it would be difficult to use with superconductors that either do not grow on another metal film or do not form good tunnel barriers. The problem of junction alignment would make measurements on quench-condensed films, for example, very hard.

More recent work[8,11,20–23] has demonstrated that charge-imbalance effects can be observed in a single superconductor–insulator–normal-metal (SIN) tunnel junction if the resistance of the junction is small enough. The single junction serves as both generator and detector. Bias voltages are very small to avoid heating. This is a convenient geometry for study of diverse materials. We presently are using this geometry to study superconducting films. We have observed that the resistance R_j of a SIN junction is reduced by supercurrents, either applied directly with a current supply or induced with a magnetic field parallel to the S film. In the present paper, we wish to lay the conceptual groundwork for later data analysis. In particular, we focus on how to extract information about electron-scattering rates, coherence factors, and the density of superconducting electrons from these measurements. Because of complicating effects such as intrinsic anisotropy in the order parameter, we will present our data elsewhere, and consider only simple, ideal, situations here.

The basic idea of how charge imbalance affects the resistance of tunnel junctions is the following.[12] In any SIN junction, a small bias voltage generates a current, which in turn generates a quasiparticle charge imbalance whose amplitude is linearly proportional to the voltage and to the charge-imbalance relaxation time τ_{Q^*}. The quasiparticle charge associated with the imbalance leaks back into the normal-metal film, reducing the total current across the junction. Experimentally, this is interpreted as an additional "nonequilibrium," resistance R_{Q^*} that is very nearly proportional to τ_{Q^*}. If the intrinsic resistance R_N of the junction is large, then R_{Q^*} is negligible, and the familiar "equilibrium" resistance $R_{\rm eq}(T)$ is observed. If R_N is small enough, then R_{Q^*} is observed in addition to $R_{\rm eq}$. Thus, the relaxation time τ_{Q^*}, which depends on the interesting coherence factors and scattering rates, can be studied via the junction resistance $R_j(T)$.

Of primary interest in this paper are the effects of pair-breaking supercurrents. These either are applied directly along the length of the S film from a current supply or they are induced with a magnetic field parallel to the S film. The effect of the currents is to shorten τ_{Q^*}, and hence reduce $R_j(T)$ in a characteristic manner that allows a determination of the relevant electron scattering rate. The decrease of τ_{Q^*} with application of a supercurrent has been observed in the three-film geometry.[19] The physics is analogous to the determination of the dephasing rate of electrons in disordered metals from magnetoresistance measurements.[25]

For illustration, we consider numerical results for two hypothetical SIN tunnel junctions and treat the results as

if they were measured data. Electron-phonon scattering in the S film is included in one junction and neglected in the other for comparison. The intrinsic resistance R_N of the latter junction is chosen to be smaller than in the first, so that the total inelastic-electron-scattering rate at T_c, which includes the proximity-effect coupling between S and N, is the same for both. Treating the calculated curves as data, we show how the general features of R_j yield information about the relevant scattering rates, coherence factors, and density of superconducting electrons. To include a realistic, albeit small, amount of pair breaking in calculating quantities such as the superconducting density of states, the parameters for S were chosen to correspond to Sn.

The results of this paper are based on the Green's-function theory of charge imbalance in tunnel junctions,[2,3,9,10] rather than the simpler Boltzmann-equation theory,[4,5] to include the effects of pair breaking on the order parameter, density of states, and coherence factors in the superconductor. Some approximations are made to simplify calculations, as discussed below. In regard to the effects of pair breaking, we note that pair-breaking effects due to intrinsic processes such as electron-phonon scattering are typically small, so the two theories give nearly the same results.[9] In such cases, pair-breaking effects become important only when the pair-breaking rate due to applied supercurrents and magnetic fields is large. In other cases—for example, superconductors containing magnetic impurities—pair-breaking effects due to the intrinsic rate may be important.

We restrict the discussion to include the effects of electron-phonon scattering, the proximity of the normal-metal film to the superconductor, and applied currents and magnetic fields. Relaxation associated with intrinsic anisotropy in the order parameter can be significant,[17,23] but is omitted here for simplicity. Electron-electron scattering,[26] scattering from magnetic impurities,[18] and the pair-breaking effect of supercurrent fluctuations[27] may also be important under some circumstances, but they are similarly omitted.

To clarify the experimental geometry and some of the assumptions inherent in the theory, the discussion begins with some considerations associated with choosing experimental parameters.

II. EXPERIMENTAL CONSIDERATIONS

A simplified experimental configuration is shown in Fig. 1. The superconducting film is deposited on a glass substrate, oxidized lightly, and masked with insulating SiO films. Then the normal-metal electrode is deposited to complete the junction. The normal-metal film is coated with a superconducting film with a relatively high T_c, such as Pb. The normal-metal film is thick and/or dirty enough that any superconductivity induced by the Pb film decays before reaching the junction insulator. The Pb film and the superconducting film form equipotentials so the current density through the junction is as uniform as possible.

Convenient parameter values that we have used are junction area 300×300 μm^2, superconducting film width

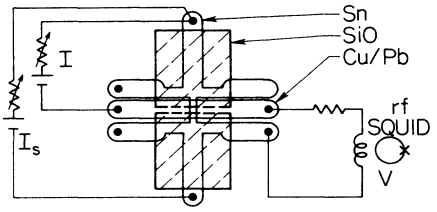

FIG. 1. Schematic sample configuration for measurement of the low-voltage resistance of a Sn/Sn-oxide/Cu SIN tunnel junction. I and V are the current and voltage in the junction; I_s is a supercurrent flowing along the S film.

300 μm, superconducting film thickness 300–800 Å, normal-metal thickness 4000 Å, SiO thickness 500 Å, and intrinsic junction resistances from 4 $\mu\Omega$ to 4 mΩ. Considerations that go into choosing these values are as follows.

(1) The intrinsic resistance R_N of the junction should be chosen so that the proximity-effect tunneling rate[12,13] $1/\tau_{tun}$ is about one-tenth of the rate of interest.

(2) The length of the superconducting strip actually in the junction should be much larger than the distance, $\lambda_{Q^*}=\sqrt{D\tau_{Q^*}}$, that a quasiparticle diffuses in a charge-imbalance relaxation time τ_{Q^*}. D is the electron-diffusion constant. This condition ensures that the charge imbalance is essentially uniform across the entire junction area, decay to zero in a length λ_{Q^*} near the edge of the junction.

(3) The superconducting film should be much thinner than both λ_{Q^*} and the Ginzburg-Landau coherence length, so that the charge imbalance and the order parameter Δ are uniform through the thickness of the film.

(4) The normal metal must be thick enough that a supercurrent cannot flow through it from the Pb film on top to the S film. However, it should be thin enough that its resistance is much less than the junction resistance.

(5) The resistance of the junction should be measured with the smallest, easily measured, voltage, typically a few hundred nanovolts. Over this range, current I is proportional to voltage V, so the resistance $R_j(T)=V/I$ is well defined. Heating is avoided.

III. NUMERICAL RESULTS AND GENERAL ANALYSIS

It is useful to discuss in general terms how useful information can be obtained from R_j as a function of temperature and of applied current or field before developing the microscopic model. For this purpose, we will consider calculated results for two hypothetical SIN junctions. The difference between the two junctions is that electron-phonon scattering in the S film is omitted for one but included for the other. To include a realistic amount of pair breaking due to inelastic processes, calculations are done using typical values for Sn for the S film. Intrinsic gap anisotropy that exists in real Sn films is omitted. For all situations illustrated in the figures, modifications due to inelastic pair breaking are a few percent or less.

For the junction that includes electron-phonon scattering, the parameters are S-film thickness $d=600$ Å, width $w=300$ μm, and resistivity $\rho=3$ $\mu\Omega$ cm, a junction area of $(300\,\mu\text{m})^2$, and an intrinsic junction resistance $R_N=100$ $\mu\Omega$. The electron-phonon scattering rate in the S film for an electron at the Fermi surface at $T=T_c=3.715$ K is about[28,29] 4×10^9 s^{-1}, and is proportional to T^3 in the normal state.[29] The proximity (tunneling) rate $1/\tau_{\text{tun}}$ that characterizes the strength of coupling between the S and N films is inversely proportional to R_N and independent of T:[12,30]

$$1/\tau_{\text{tun}}=1/2N(0)e^2\Omega R_N\approx4\times10^8\ \text{s}^{-1}\ , \tag{1}$$

for the present junction, with a density of states[31] $2N(0)=2.9\times10^{28}$ eV^{-1} m^3, and an injected volume $\Omega=(300\ \mu\text{m})^2\times600$ Å. Note that the tunneling process acts like an inelastic scattering process in parallel with electron-phonon scattering so that the total inelastic scattering rate is their sum. For this example junction, $1/\tau_{e\text{-ph}}(T_c)$ is about 10 times larger than $1/\tau_{\text{tun}}$, and will dominate the charge-imbalance relaxation process down to $T/T_c\approx0.5$, where $1/\tau_{e\text{-ph}}\approx0.5^3/\tau_{e\text{-ph}}(T_c)\approx1/\tau_{\text{tun}}$.

For the junction that does not include electron-phonon scattering in the S film, the parameters are the same, except that R_N is 11 times smaller, so that the tunneling rate is $1/\tau_{\text{tun}}=4.4\times10^9$ s^{-1}. Thus, the total inelastic scattering rate at T_c is 4.4×10^9 s^{-1} in both junctions.

The calculated resistances $R_j(T)/R_N$ for these junctions is shown in Fig. 2. The "equilibrium" resistance

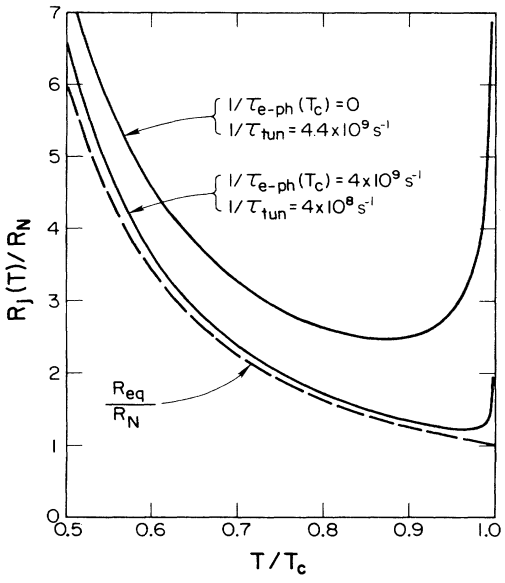

FIG. 2. Calculated normalized junction resistance $R_j(T)/R_N$ vs T/T_c for two hypothetical SIN tunnel junctions. $T_c=3.715$ K was used for the S film. Electron-phonon scattering is included in the S film for one junction but not for the other. $R_{\text{eq}}(T)/R_N$ is the normalized equilibrium resistance of the junction. The difference between R_j and R_{eq} is the nonequilibrium resistance R_{Q^*} associated with a charge imbalance in the S film. As seen in the figure, the addition of electron-phonon scattering to tunneling relaxation reduces $R_j(T)/R_N$ by reducing R_{Q^*}.

$R_{\text{eq}}(T)/R_N$ is the resistance the junction would have if nonequilibrium effects were negligible. Although it nominally was calculated for $1/\tau_{\text{tun}}=4.4\times10^9$ s^{-1} and $T_c=3.715$ K, i.e., $\hbar/k_BT_c\tau_{\text{tun}}=0.009$, the curve labeled $1/\tau_{e\text{-ph}}=0$ is a limiting curve that is independent of $1/\tau_{\text{tun}}$ as long as $\hbar/\tau_{\text{tun}}\ll k_BT$ and Δ. Values of $R_j(T)/R_N$ for junctions with $0<1/\tau_{e\text{-ph}}(T_c)<10/\tau_{\text{tun}}$ lie between the two curves in Fig. 2. Close inspection of Fig. 2 reveals that the two $R_j(T)/R_N$ curves are merging as T decreases and electron-phonon scattering freezes out.

To see in more detail how the scattering rates influence $R_j(T)$, consider the calculated curves as data. From $R_j(T)$ near T_c, we can obtain R_N and the rates $1/\tau_{\text{tun}}$ and $1/\tau_{e\text{-ph}}(T_c)$. Near T_c, $R_{\text{eq}}(T)\approx R_N$ is nearly constant compared with $R_{Q^*}(T)$, which diverges as k_BT_c/Δ, where Δ is the order parameter. By fitting $R_j(T)$ near T_c with the form

$$R_j(T)\approx R_N+\frac{4k_BT}{\pi\Delta}\frac{\tau_{\text{in}}}{2N(0)e^2\Omega}\ , \tag{2}$$

we obtain both R_N and the rate

$$1/\tau_{\text{in}}=1/\tau_{\text{tun}}+1/\tau_{e\text{-ph}}(T_c)\ .$$

From R_N and measured sample parameters, $1/\tau_{\text{tun}}$ is calculated, then subtracted from $1/\tau_{\text{in}}$ to give $1/\tau_{e\text{-ph}}(T_c)$. This procedure has been used successfully even in very low resistance junctions.[20–23] The factor $\pi\Delta/4k_BT$ is essentially an average over energy of the coherence factor for charge-imbalance relaxation due to inelastic electron scattering near T_c. If an elastic process were dominant, then the coherence factor would be proportional to $(\Delta/k_BT)^2$.[5]

Away from T_c, it is difficult to extract information from $R_j(T)$ since both $R_{\text{eq}}(T)$ and $R_{Q^*}(T)$ depend on T. Measurements of R_j as a function of supercurrent along the S strip or of magnetic field parallel to the S strip, are very useful. In the present examples, we will see that these measurements allow determinations of the electron-phonon scattering rate and the density of superconducting electrons as functions of T below T_c. The procedure works because the nonequilibrium resistance $R_{Q^*}(T)$ is much more sensitive than $R_{\text{eq}}(T)$ to external pair-breaking perturbations such as a supercurrent I_s along the superconducting strip or a magnetic field $B_\parallel$ parallel to the strip, so measurements at low fields and currents probe R_{Q^*} almost exclusively.

The experimental arrangement for measuring $R_j(T,I_s)$ is illustrated in Fig. 1. The current I through the junction is fixed, and the voltage V across the junction is measured while the current I_s along the superconducting film is increased. The effect of the supercurrent is to shorten the charge-imbalance relaxation time τ_{Q^*}, and thereby to reduce R_{Q^*}. The equilibrium resistance is also reduced. Measurements of $R_j(T,B_\parallel)$ as a function of magnetic field $B_\parallel$ are made in a similar fashion, but the external current passes through a solenoid around the sample rather than along the superconducting film.

Figure 3 shows calculated values of $R_j(T,B_\parallel)/R_N$ and $R_{\text{eq}}(T)/R_N$ versus magnetic field for several temperatures. The divergence in R_j/R_N evident in Fig. 3(a) occurs as

the field approaches the critical field, and the order parameter vanishes. In other words, the resistance diverges as $T \rightarrow T_c(B_\parallel)$ just as it diverges when $T \rightarrow T_c$ in zero field, as shown in Fig. 2. This divergence has not been observed due to the large fields required, but would be interesting to study because it would give a more accurate value for the critical field than determinations based on resistance measurements.

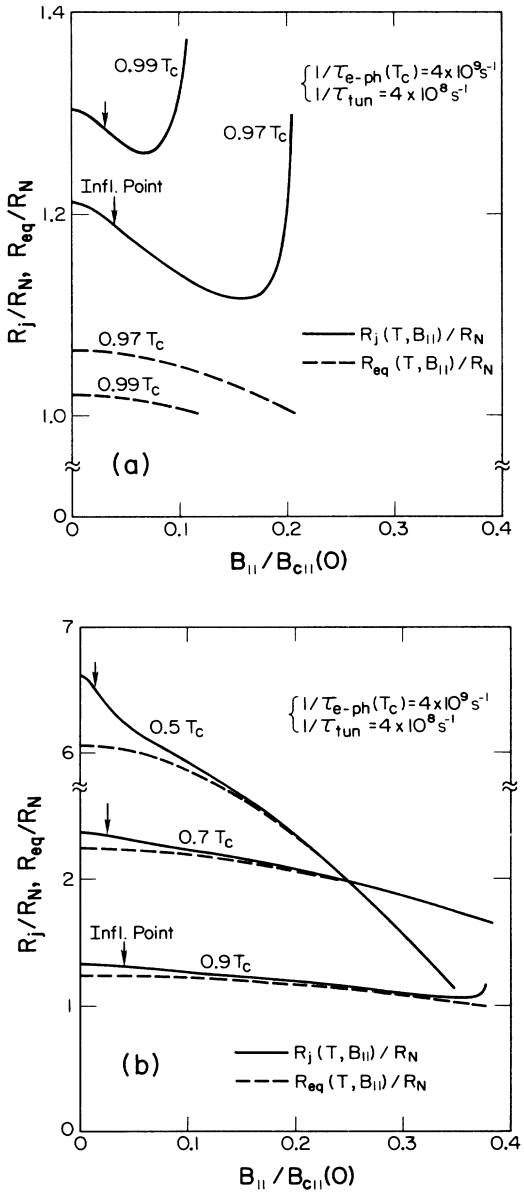

FIG. 3. Calculated resistances $R_j(T,B_\parallel)/R_N$ and $R_{eq}(T,B_\parallel)/R_N$ vs $B_\parallel/B_{c\parallel}(0)$ at several temperatures for a hypothetical SIN junction including electron-phonon scattering in the S film. $B_\parallel$ is the magnetic field applied parallel to the S film and $B_{c\parallel}(0)$ is the critical field at $T=0$. $T_c=3.715$ K was used for the S film. The vertical arrows mark the low-field inflection points. (a) Results near T_c showing the divergence in R_j/R_N as $B_\parallel$ approaches $B_{c\parallel}(T)$, and hence $T/T_c(B_\parallel)\rightarrow 1$. (b) Results away from T_c. Note the change in vertical scale for $T/T_c=0.5$. The solid curves for R_j/R_N are terminated before the critical field for clarity.

In practice, the low-field portion of the curves in Fig. 3 are measured. If they were data on an ideal BCS superconductor, then careful numerical fits to the theory presented below would yield all the information desired about electron scattering rates and coherence factors. Since the most interesting applications of this technique will be to materials in which one is unsure of the correct microscopic model, e.g., disordered superconductors in which electron-electron scattering may be important, it is useful to dissect the calculated curves to see how their general features can be used to infer the microscopic physics. We have found that this sort of crude analysis of data offers a starting point for more detailed fitting.

As seen in Fig. 3, for small fields R_{eq}/R_N is nearly constant. The dominant effect of the field is to reduce R_{Q^*}/R_N. The inflection point in $R_j(B_\parallel)/R_N$ is marked with an arrow because its location allows a convenient parametrization of the entire low-field curve. As one might guess, the inflection point occurs when the pair-breaking rate $1/\tau_s$ due to the field reaches a characteristic value, which turns out to be roughly half of the intrinsic pair-breaking rate. This relationship can be demonstrated near T_c by the following argument.

Consider the case in which the intrinsic pair breaking is due entirely to inelastic processes so that the intrinsic pair-breaking rate is one-half of the total inelastic scattering rate. The argument is easily generalized to include intrinsic elastic pair-breaking processes. Schmid and Schön[2] showed that, near T_c, $1/\tau_{Q^*}$ depends on the geometric mean of the total pair-breaking rate $1/2\tau_{in}+1/\tau_s$ and the inelastic pair-breaking rate $1/2\tau_{in}$:

$$\frac{1}{\tau_{Q^*}} \approx \frac{\pi\Delta}{4k_BT}\left[\left[\frac{1}{2\tau_{in}}+\frac{1}{\tau_s}\right]\frac{1}{2\tau_{in}}\right]^{1/2} . \tag{3}$$

[This result is modified extremely close to T_c where the dynamic charge-imbalance relaxation rate, in large square brackets in Eq. (3), becomes larger than the frequency $\Delta/\hbar$. We are not concerned with this range here.] In the present case, the inelastic rate is $1/\tau_{in}=1/\tau_{tun}+1/\tau_{e\text{-ph}}$, and the elastic pair-breaking rate $1/\tau_s$ is[32]

$$1/\tau_s = B_\parallel^2 d^2/12\rho N(0)\hbar^2 . \tag{4}$$

Not too close to T_c, the dependence of Δ on $1/\tau_s$ is small, and $\tau_{Q^*}(B_\parallel)$ versus $B_\parallel$ has an inflection point at $1/\tau_s \approx 1/4\tau_{in}$, i.e.,

$$B_\parallel^2 \mid_{infl} d^2/12\rho N(0)\hbar^2 \approx \tfrac{1}{4}(1/\tau_{tun}+1/\tau_{e\text{-ph}}) . \tag{5}$$

To the extent that $R_{Q^*}(T)$ is proportional to τ_{Q^*} and $R_{eq}(T)$ is unaffected by the relevant fields, the inflection point in R_j/R_N coincides with that in τ_{Q^*}, and serves as a crude indicator of the inelastic scattering rate.

Figure 4 shows normalized values of $1/\tau_s$ at the low-field inflection point in R_j/R_N versus $B_\parallel$ for example junctions with and without electron-phonon scattering. [Plots of R_j/R_N versus $B_\parallel/B_{c\parallel}(0)$ for the junction with no electron-phonon scattering are shown below.] For the junction including electron-phonon scattering, $\tau_s^{-1} \mid_{infl}$

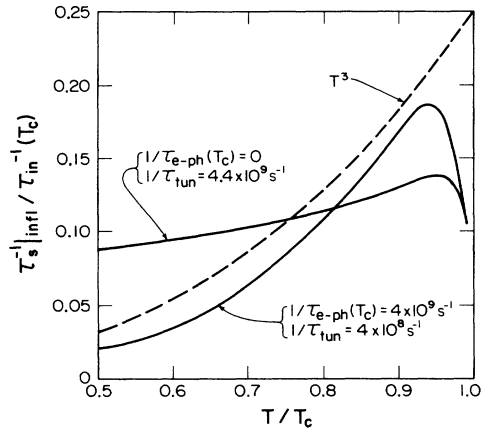

FIG. 4. The normalized elastic pair-breaking rate $\tau_s^{-1}|_{\text{infl}}/\tau_{\text{in}}^{-1}(T_c)$ at the low-field inflection point in $R_j(B_\parallel)/R_N$ vs $B_\parallel$ for the two example junctions. Curves are shown for junctions with and without electron-phonon scattering and with the same inelastic scattering rate at T_c, 4.4×10^9 s^{-1}. Including electron-phonon scattering results in a strong T dependence roughly paralleling the T^3 dependence of the electron-phonon scattering rate in the normal state.

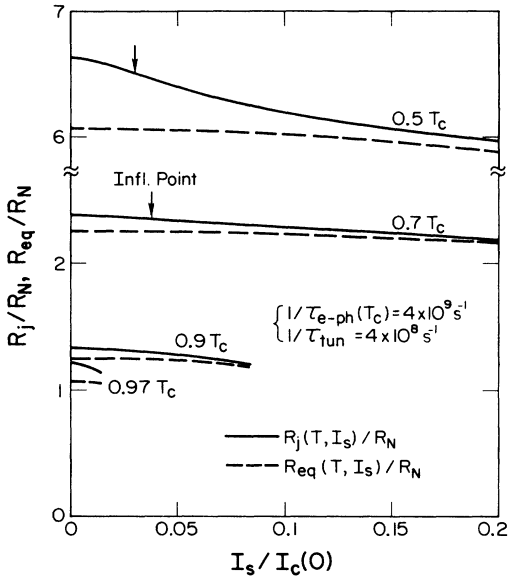

FIG. 5. Calculated resistances $R_j(T,I_s)/R_N$ and $R_{\text{eq}}(T,I_s)/R_N$ vs $I_s/I_c(0)$ at several temperatures for the same SIN junction as in Fig. 3. I_s is the supercurrent along the S film and $I_c(0)$ is the critical current at $T=0$. The vertical arrows mark the low-current inflection points. In contrast to results in a magnetic field, Fig. 3, there is no divergence at $I_c(T)$ because Δ is not depressed to 0 at I_c.

rises by a factor of about 8 between $T/T_c=0.5$ and 0.9, reflecting the T^3 dependence of $1/\tau_{e\text{-ph}}$ in the normal state. As expected, the dependence of Δ on $1/\tau_s$ keeps $\tau_s^{-1}|_{\text{infl}}/\tau_{\text{in}}^{-1}(T_c)$ from reaching $\frac{1}{4}$ at T_c. For the junction with no electron-phonon scattering, $\tau_s^{-1}|_{\text{infl}}$ is roughly constant, as expected from the T-independent rate $1/\tau_{\text{tun}}$. The value of $\tau_s^{-1}|_{\text{infl}}/\tau_{\text{in}}^{-1}(T_c)$ is much smaller than $\frac{1}{4}$ for this case because the proportionality between $R_{Q^*}(T)$ and τ_{Q^*} is worst when tunneling is the only charge-imbalance relaxation process, as is shown below.

The possibility of obtaining electron scattering rates from R_j in this way is a major result of this paper. The result should be somewhat insensitive to junction quality. In real junctions imperfections in the junction insulator might change the magnitude of $R_{Q^*}(T)$, but probably not change its dependence on $B_\parallel$, e.g., the value of $1/\tau_s$ at the inflection point.

The density of superconducting electrons $n_s(T)$ can be obtained from $R_j(T,I_s)/R_N$ versus supercurrent I_s. Calculated curves for $R_j(T,I_s)/R_N$ are shown in Fig. 5 for the SIN junction including electron-phonon scattering. The inflection point at low current has a very strong temperature dependence, in contrast to the field measurements in Fig. 3. The reason is that the pair-breaking rate for a current I_s depends on $n_s(T)$, whereas the pair-breaking rate due to a given field is independent of T. Once again, at the inflection point, the external pair-breaking rate[32] is about one-fourth of the inelastic scattering rate:

$$\frac{2\gamma^2\rho}{\pi^4 2N(0)(k_BT_c)^2d^2w^2}\frac{n_s(0)^2}{n_s(T)^2}I_s^2|_{\text{infl}} \approx \frac{1}{4}\left[\frac{1}{\tau_{\text{tun}}}+\frac{1}{\tau_{e\text{-ph}}}\right]. \quad (6)$$

where $\pi/\gamma=1.765$. This expression for the pair-breaking rate due to an applied supercurrent is valid in the dirty limit and for I_s much less than the critical current $I_c(T)$. Since the rate on the right-hand side (rhs) of Eq. (6) is determined from the field measurements, the density $n_s(T)/n_s(0)$ is determined from

$$\frac{n_s(T)}{n_s(0)}=\frac{I_s|_{\text{infl}}}{B_\parallel|_{\text{infl}}}\frac{2\sqrt{3}\gamma\rho\hbar}{\pi^2d^2wk_BT_c}. \quad (7)$$

The density of states has cancelled out, leaving only measurable parameters and constants.

IV. THEORY OF THE RESISTANCE OF SIN TUNNEL JUNCTIONS

The above discussion has shown how the general features of R_j can be used to obtain useful information. Of course, with real data, detailed numerical fits will yield more precise values for the various rates. The basic concepts needed for such calculations are outlined in this section, which adapts the theory of charge imbalance to SIN junctions. The principal contribution to the literature of this formulation is that it includes the proximity-effect coupling between the S and N films.

A. Background and assumptions

We consider a SIN junction in which the superconducting film is sufficiently thin, and the areal dimensions of the junction sufficiently large, that quasiparticle diffusion

ensures a uniform nonequilibrium quasiparticle distribution throughout the volume of superconductor adjacent to the insulator. The relevant diffusion length is $\lambda_{Q^*}=\sqrt{D\tau_{Q^*}}$, where $1/\tau_{Q^*}$ is the charge-imbalance relaxation rate, $D=v_F l/3$ is the electron diffusion constant, v_F is the Fermi velocity, and l is the electron mean-free path that is measured by the normal-state residual resistivity.

The discussion is restricted to junctions biased at very low voltages, $|eV| \ll k_B T$ and $\Delta(T)$. Heating can be neglected, since it is proportional to V^2. The nonequilibrium quasiparticle distribution in the superconducting film is a pure charge imbalance; that is, quasiparticles are added on one side of the Fermi surface and removed from the other side such that the total number of quasiparticles remains constant. In this case, the magnitude of Δ is unaffected by the quasiparticle disequilibrium; only the phase of Δ changes.[2,4]

We basically follow the dirty-limit, Green's function formulation of the problem,[2,9,10] adapting the theory to SIN junctions to properly include the proximity effect coupling between the S and N films through the insulator. Equations are cast in a form that emphasizes their relation to the Boltzmann-equation picture developed by Pethick and Smith.[4,5]

The order parameter $\Delta(T, 1/\tau_s, 1/\tau_{in})$ is calculated following Maki.[32] Since we consider only cases in which the inelastic pair-breaking rate is small compared with T_c, we treat the inelastic rate like an elastic pair breaker in calculating Δ. For large inelastic rates, the full Eliashberg equations would be required.[9,10] The density of superconducting electrons $n_s(T, 1/\tau_s, 1/\tau_{in})$ also is calculated according to Maki,[32] with inelastic pair-breaking treated the same as elastic. The superconducting density of states $N_1(E)$ and the other functions N_2, R_1, and R_2 that are needed to calculate the effective quasiparticle charge $q(E)$ and coherence factors are calculated from Eqs. (17), (19), and (34) of Ref. 9. Checks on our computer programs are described in the Appendix.

B. Formal calculation of $R_j(T)$

The main purposes of this section are to show that R_j is the sum of the usual equilibrium resistance $R_{eq}(T)$ and a nonequilibrium resistance $R_{Q^*}(T)$, and to relate $R_{Q^*}(T)$ to the charge-imbalance relaxation time τ_{Q^*}. We consider only the dirty limit, in which the momentum distribution of quasiparticles is isotropic, so that quasiparticle states can be labeled by energy E. As usual,[1,2,4,5,9,10] the tunnel junction is described by the tunneling Hamiltonian with a tunneling probability that is independent of energy.

The quasiparticle distribution function in the superconductor is written

$$f_E = f^0(E) + \delta f_E \ , \tag{8}$$

where $f^0(E)$ is the Fermi function with argument $E/k_B T$, and δf_E is the nonequilibrium part of the distribution function. The quasiparticles in the normal-metal electrode are assumed to be in equilibrium. E is measured relative to the actual, nonequilibrium, chemical potential μ_s in the superconductor.

[There is a difference in the meaning of δf_E in the Green's-function and Boltzmann-equation theories, as discussed in Appendix A of Ref. 9. In the former, f_E evolves into the probability of finding an electron as T increases past T_c, whereas in the latter f_E evolves into the probability of finding a normal excitation, i.e., an electron above the Fermi surface and a hole below. For a charge-imbalance disequilibrium, in the Green's-function theory δf_E is symmetric about the Fermi surface, while in the Boltzmann-equation theory δf_E is antisymmetric about the Fermi surface. To avoid confusion in the interpretation of relations given below, we note that the important quantity here is the charge associated with nonequilibrium excitations, i.e., the product of δf_E and the effective quasiparticle charge $q(E)$. The product $q\delta f_E$ for a charge-imbalance disequilibrium is symmetric about the Fermi surface in both theories.]

Q^* is the number density of electrons associated with excitations. Q^* is zero in thermal equilibrium, where $f_E = f^0(E)$. If a disequilibrium exists, then

$$Q^* = 4N(0)\int_0^\infty dE\, N_1(E) q(E) \delta f_E \ . \tag{9}$$

Extension of the limit of integration to infinity assumes that the width of the conduction band is much larger than $k_B T$, since δf_E is substantial only within $k_B T$ of the Fermi surface.

Since $q(E)$ and $N_1(E)$ play important roles, it is worthwhile to pause here to examine how they depend on energy and pair-breaking rates. Following the notation of Refs. 9 and 10, we define normalized elastic and inelastic pair-breaking rates $\Gamma_s = \hbar/\tau_s\Delta$ and $\Gamma = \hbar/2\tau_{in}\Delta$. The functions N_1, N_2, R_1, and R_2 are calculated from Eqs. (17), (19), and (34) of Ref. 9, with the approximations $\mathrm{Im}(ZE) = \Gamma\Delta$ and $\phi = \Delta$, thus neglecting strong-coupling effects on Δ while retaining the broadening of excitation energy levels due to inelastic scattering. In the same notation, $q(E) = (N_1^2 - R_2^2)/N_1$, as seen from a comparison of Eq. (4.3) of Ref. 9 and Eq. (9) above. In the BCS limit of small pair breaking, $\Gamma + \Gamma_s \ll 1$, and, for $E > 0$,

$$q(E) = (E^2 - \Delta^2)^{1/2}/E \ , \tag{10}$$

$$N_1(E) = E/(E^2 - \Delta^2)^{1/2} \ , \tag{11}$$

so that as $E \to 0$, $q \to 0$ and $N_1 \to \infty$ such that $N_1(E)q(E) = 1$.

Figure 6 shows $q(E)$ and $N_1(E)$ for different amounts of elastic pair breaking. E is normalized to the value of Δ in the absence of pair breaking. Values of Γ and Γ_s are for the example junctions at $T/T_c \approx 0.9$, and for $1/\tau_s = 0$ and $1/\tau_s \approx 4/\tau_{in}$. Note that the gap edge is lowered by increased elastic pair breaking. For both cases illustrated, $q(E)$ rises from zero at the gap edge to 1 at high energies, as the nature of excitations evolves from an equal mixture of electron and hole, to pure electron.

The junction resistance $R_j(T)$ is obtained by calculating the current I that flows in the presence of a bias voltage V. The sign convention used here is that when V is positive, electrons flow from N to S, so that Q^* is positive. From Eqs. (4.5) and (4.6) in Ref. 10, we find

$$I = V g_{NS}(T)/R_N - Q^*/2N(0)|e|R_N \ , \tag{12}$$

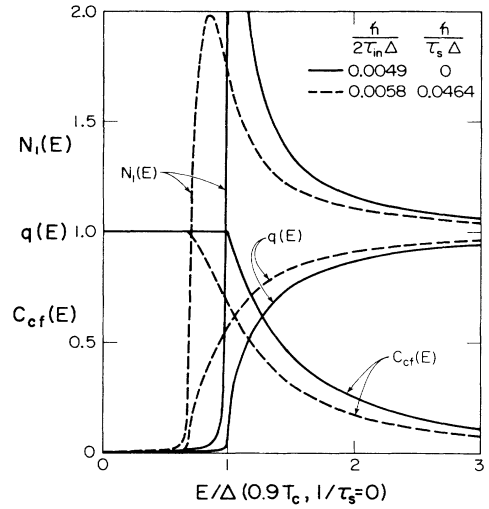

FIG. 6. Normalized density of states $N_1(E)$, effective quasiparticle charge $q(E)$, and the coherence factor $C_{cf}(E)$ for elastic charge-imbalance relaxation processes, vs $E/\Delta(0.9T_c, 1/\tau_s=0)$. The solid curves are calculated for no external elastic pair breaking, and for an internal inelastic pair-breaking rate appropriate to Sn at $T\approx 0.9T_c$. They are very close to the BCS results, Eqs. (10) and (11), because the internal rate is small compared with Δ. The dashed curves are calculated for an elastic pair-breaking rate 8 times larger than the internal inelastic pair-breaking rate. The depression in Δ is calculated for Sn at $T\approx 0.9T_c$.

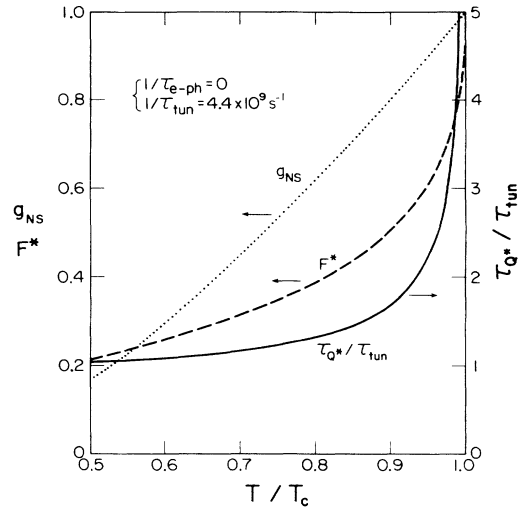

FIG. 7. Calculated, normalized charge-imbalance relaxation time τ_{Q^*}/τ_{tun} vs T/T_c for a SIN junction with no electron-phonon scattering in the S film. Also shown are F^* and the normalized conductance g_{NS}. Pair-breaking effects are small for the temperature range shown.

$$g_{NS}(T)\equiv 2\int_0^\infty dE\, N_1(E)\left[\frac{-\partial f^0(E)}{\partial E}\right], \tag{13}$$

where R_N is the intrinsic resistance of the junction. From Eq. (12), $R_N/g_{NS}(T)$ is the equilibrium resistance $R_{eq}(T)$ of the junction, i.e., the resistance when Q^* is negligible. As shown in Fig. 7 for the case of a small pair-breaking rate, g_{NS} is 1 at T_c and decreases monotonically as T decreases. Equation (12) shows that the charge imbalance Q^* reduces the total current. This leads ultimately to the nonequilibrium resistance R_{Q^*}.

Before calculating $R_{Q^*}(T)$, we pause to consider what voltage V the voltmeter across the junction reads. Keeping track of electric and chemical potentials is tricky in detail, but the end result is simple: the voltmeter measures the electrochemical potential difference between the electrons in N and the superconducting electrons in S.[33] There is a chemical-potential shift in the injected region of the superconductor because bulk charge neutrality requires that when the quasiparticle electron density increases from 0 to Q^*, the condensate density decreases by the same amount. This requires a shift $\delta\mu_s$ in the condensate chemical potential such that

$$2N(0)\delta\mu_s + Q^* = 0\ . \tag{14}$$

This is consistent with the voltmeter measuring the line integral of the electric field because there is an electric field in the S film at the edges of the junction where the charge imbalance decays to zero. The electric field in the film is required to keep the condensate electrochemical potential constant throughout the S film, as it is in steady state. The end result is that the voltmeter reads the sum of the two electric potential drops, which equals the electrochemical potential drop across the junction. This potential is larger in magnitude than the electric potential alone.

Now we can define the charge-imbalance relaxation rate $1/\tau_{Q^*}$ and calculate $R_{Q^*}(T)$. The total current I in Eq. (12) should be thought of as the difference between a forward "equilibrium" current proportional to the electrostatic potential $[V-Q^*/2N(0)|e|]$ (with magnitude less than $|V|$) across the junction, and a reverse "nonequilibrium" current proportional to the chemical potential drop $Q^*/2N(0)|e|$ across the junction, i.e.:

$$I = I_{eq} - I_{Q^*}\ , \tag{15}$$

$$I_{eq} = [V - Q^*/2N(0)|e|]g_{NS}/R_N\ , \tag{16}$$

$$I_{Q^*} = [Q^*/2N(0)|e|](1-g_{NS})/R_N\ . \tag{17}$$

The reverse current I_{Q^*} represents tunneling of quasiparticle charge from S to N through the tunnel barrier. The physical meaning of the separation of I into two parts is that the electrostatic potential across the junction is the applied perturbation, and the chemical-potential shift, or charge imbalance, is the response of the junction to the perturbation.

Now consider the total rate $G_{tun}(E)$ at which quasiparticles are generated at each energy E, i.e., the rate at which $N_1(E)\delta f_E$ is replenished by tunneling electrons. From Eq. (4.10) in Ref. 10, in the limit $|eV| \ll k_B T$,

$$G_{tun}(E) = N_1(E)q(E)\left[\frac{-\partial f^0(E)}{\partial E}\right]|e|\,V/\tau_{tun} - N_1(E)\delta f_E/\tau_{tun}\ . \tag{18}$$

Analogously to the division of the current, we divide $G_{\rm tun}(E)$ into equilibrium and nonequilibrium parts proportional to the electrostatic and chemical potentials:

$$G_{\rm tun}(E)=G_{\rm tun,eq}(E)-G_{\rm tun,Q^*}(E)\ , \tag{19}$$

$$G_{\rm tun,eq}(E)=N_1(E)q(E)\left[\frac{-\partial f^0(E)}{\partial E}\right]$$

$$\times[\,|e|V-Q^*/2N(0)]/\tau_{\rm tun}\ , \tag{20}$$

$$G_{\rm tun,Q^*}(E)=-N_1(E)q(E)\left[\frac{-\partial f^0(E)}{\partial E}\right][Q^*/2N(0)\tau_{\rm tun}]$$

$$+N_1(E)\delta f_E/\tau_{\rm tun}\ . \tag{21}$$

The notation used here differs slightly from Ref. 13. Generation and relaxation rates here are larger than those in Ref. 13 by a factor of N_1 since Ref. 13 deals with an equation for δf_E rather than $N_1\delta f_E$.

We define the charge-imbalance generation rate, $dQ^*/dt\,|_{\rm gen}$, to be the rate at which quasiparticles are generated by only the equilibrium part of $G_{\rm tun}$ times the charge each carries:

$$\left.\frac{dQ^*}{dt}\right|_{\rm gen}=4N(0)\int_0^\infty dE\,q(E)G_{\rm tun,eq}(E)\ . \tag{22}$$

The fraction of the "equilibrium" current of electron charge to enter the superconductor as quasiparticle charge is commonly denoted F^*, and from Eqs. (13), (16), (20), and (22),

$$F^*\equiv\int_0^\infty dE\,N_1q^2\left[\frac{-\partial f^0}{\partial E}\right]\Big/\int_0^\infty dE\,N_1\left[\frac{-\partial f^0}{\partial E}\right]\ . \tag{23}$$

The rest of the current goes directly into the condensate. F^* lies between 0 and 1, decreasing monotonically from 1 as T decreases from T_c as shown in Fig. 7. Both F^* and g_{NS} have been discussed previously for the case of no pair breaking.[34] It is convenient to write the charge-imbalance generation rate in terms of F^* and g_{NS}:

$$\left.\frac{dQ^*}{dt}\right|_{\rm gen}=2N(0)[\,|e|V-Q^*/2N(0)]F^*g_{NS}/\tau_{\rm tun}\ . \tag{24}$$

The charge-imbalance relaxation rate is the generation rate divided by the steady-state value of Q^*,

$$\frac{1}{\tau_{Q^*}}=\left.\frac{dQ^*}{dt}\right|_{\rm gen}\Big/Q^* \tag{25}$$

$$=[2N(0)\,|e|V/Q^*-1]F^*g_{NS}/\tau_{\rm tun}\ . \tag{26}$$

For low voltages, $Q^*\propto V$, so $1/\tau_{Q^*}$ is independent of V.

Finally, to relate $R_j(T)$ and $1/\tau_{Q^*}$, solve Eqs. (24) and (25) for Q^* in terms of τ_{Q^*}, and use the result in Eq. (12) for I to obtain

$$R_j(T)=R_{\rm eq}(T)+R_{Q^*}(T)\ , \tag{27}$$

$$R_{\rm eq}(T)=R_N/g_{NS}(T)\ , \tag{28}$$

$$R_{Q^*}(T)=R_{\rm eq}(T)/[\tau_{\rm tun}/F^*\tau_{Q^*}-(1-g_{NS})]\ . \tag{29}$$

Equation (29) is an important result of this paper. From Eq. (29), $R_{Q^*}(T)$ would be proportional to τ_{Q^*}, as expected, if the factor $1-g_{NS}$ were much smaller than $\tau_{\rm tun}/F^*\tau_{Q^*}$. It often is smaller. In particular, it is much smaller in the usual situation in which $1/\tau_{Q^*}$ is determined by a rate much larger than $1/\tau_{\rm tun}$ as in the example junction that includes electron-phonon scattering. The proportionality is worse when the only charge-imbalance relaxation process is the tunneling process. This case is discussed in Sec. IV D below. When $1-g_{NS}$ can be neglected, $R_{Q^*}(T)$ can be written

$$R_{Q^*}(T)\approx R_{\rm eq}(T)F^*\tau_{Q^*}/\tau_{\rm tun}\quad(1-g_{NS}\ \text{negligible})\ . \tag{30}$$

It is physically reasonable that R_{Q^*} is proportional to the fraction F^* of the equilibrium current to enter the superconductor as quasiparticle charge, since the charge-imbalance generation rate is proportional to F^*. (If $1/\tau_{Q^*}$ were defined using $I_{\rm eq}$ in place of $dQ^*/dt\,|_{\rm eq}$, in the spirit of Schmid and Schon,[2] then the factor of F^* would be absorbed into τ_{Q^*} and not appear explicitly.) The approximate result (30) is at the heart of the rough analysis in Sec. III above.

C. "Boltzmann" equation for δf_E

To calculate R_{Q^*}, we need to know τ_{Q^*}, so we need to know δf_E. The "Boltzmann" equation for a steady-state, spatially uniform perturbation has the form[2–5,9,10]

$$0=G_{\rm tun}(E)-G_s(E)-G_{e\text{-ph}}(E)\ . \tag{31}$$

$G_{\rm tun}(E)$ has already been discussed. $G_s(E)$ is the net rate at which quasiparticles scatter elastically across the Fermi surface in the presence of applied supercurrents and fields. $G_{e\text{-ph}}(E)$ is the net rate at which quasiparticles scatter from state E to all other states E' due to absorption or emission of phonons.

For the situations considered here, the scattering term $G_s(E)$ arises from elastic scattering from nonmagnetic impurities in the presence of a supercurrent, either an applied supercurrent or a supercurrent induced by an applied magnetic field. $G_s(E)$ is related to δf_E through[10]

$$G_s(E)=(1/\tau_s)C_{cf}(E)N_1(E)(2N_1\delta f_E)\ , \tag{32}$$

$$1/\tau_s=Dp_s^2/2\hbar^2+De^2B_\parallel^2d^2/6\hbar^2 \tag{33}$$

$$=\frac{2\gamma^2\rho}{\pi^4 2N(0)(k_BT_c)^2d^2w^2}\frac{n_s(0)^2}{n_s(T,1/\tau_s)^2}I_s^2$$

$$+\frac{B_\parallel^2d^2}{12\rho N(0)\hbar^2}\ , \tag{34}$$

when free-electron relations among D, ρ, and $2N(0)$ are used. p_s is the superfluid momentum, $2mv_s$. Note that n_s

depends on I_s for I_s close to the critical current I_c. We calculate the coherence factor $C_{cf}(E)$ for the elastic charge-imbalance relaxation following Eq. (4.14) in Ref. 10. In the BCS limit of small pair-breaking,[2,5]

$$C_{cf}(E)=\Delta^2/E^2 , \tag{35}$$

so it decreases monotonically from unity at the gap edge. Figure 6 shows that with or without pair breaking the coherence factor is unity at the gap edge and decreases smoothly as energy increases.

Simple elastic scattering contributes to charge-imbalance relaxation when a supercurrent flows because the supercurrent spoils the symmetry between equal-energy excitations above and below the Fermi surface by making the order parameter Δ different for different directions of momentum. This makes the coherence factor nonzero, and allows simple elastic scattering to scatter excitations across the Fermi surface. In the dirty limit, the pair-breaking rate is proportional to the elastic scattering time, not the rate, because of the strong tendency of elastic scattering to make the order parameter isotropic in spite of the current.

The term $G_{e\text{-ph}}(E)$ represents inelastic scattering of quasiparticles from phonons. There are eight basic terms. A quasiparticle can (1) absorb a phonon and stay on the same side of the Fermi surface, or (2) cross the Fermi surface; (3) emit a phonon and stay on the same side of the Fermi surface, or (4) cross the Fermi surface; (5) recombine with a quasiparticle on the same side of the Fermi surface, or (6) with one on the other side. Also, two quasiparticles can be created by absorption of a phonon, with quasiparticles created (7) on the same side of the Fermi surface, or (8) on both sides. Processes (2), (4), (5), and (7) are especially effective in relaxing a charge imbalance, but in any of these processes, the net quasiparticle charge generally changes, depending on the initial and final quasiparticle states. For the calculations presented here, the electron-phonon coupling function, $\alpha^2F(\omega)$, is assumed to be proportional to ω^2. This results from an energy-independent matrix element and a Debye density of phonon states proportional to ω^2. These terms have been discussed in detail by several authors[3,4,6,28] and are not discussed further here.

The characteristic rate associated with electron-phonon scattering, $1/\tau_{e\text{-ph}}(T_c)$, is the electron-phonon scattering rate of a quasiparticle at the Fermi surface, $E=0$, evaluated at $T=T_c$:[2]

$$1/\tau_{e\text{-ph}}(T_c)=14\pi\zeta(3)\alpha^2F(k_BT_c/\hbar)k_BT_c/\hbar\propto T_c^3 , \tag{36}$$

where $\zeta(3)\approx 1.202$ is the Riemann zeta function. At temperatures below T_c, a characteristic electron-phonon rate can be estimated from the value at T_c by using T^3 as a rough guess for its dependence on T. In the superconducting state, there is no standard definition for the rate. A detailed numerical analysis of measurements of R_j will yield $\alpha^2F(\omega)$, which can then be compared with measurements in the normal state.

The strategy for calculating $R_j(T)/R_N$ numerically is to solve Eq. (31) for $N_1\delta f_E/V$, calculate Q^*/V from Eq. (9), and finally calculate R_j/R_N from Eq. (12). $R_{eq}(T)/R_N=1/g_{NS}$ is calculated by using the definition, Eq. (13), and the density of states calculated with pair-breaking effects included.

D. Proximity effect only

In this subsection we discuss a junction in which the dominant internal charge-imbalance relaxation mechanism is the tunneling process. This limit can be realized in very low resistance junctions in which $1/\tau_{tun}$ is much larger than the electron-phonon scattering rate at all relevant energies and temperatures. The equation for δf_E is no longer an integral equation:

$$G_{tun}(E)-G_s(E)=0 . \tag{37}$$

It is worthwhile to explore this limit in detail because it is easy to solve and therefore provides a particularly clear example illustrating the basic concepts. Some results for this limit were shown in Figs. 2 and 4.

First, consider the case where there is no supercurrent. The solution for $N_1\delta f_E$ is

$$N_1\delta f_E=N_1(E)q(E)\left[\frac{-\partial f^0}{\partial E}\right]|e|V$$

$$=N_1q(|e|V/k_BT)/4\cosh^2(E/2k_BT) . \tag{38}$$

With the definition of Q^* and the above solution for δf_E, we can solve for Q^* and $1/\tau_{Q^*}$ in terms of the functions F^* and g_{NS}:

$$Q^*=2N(0)F^*g_{NS}|e|V , \tag{39}$$

$$1/\tau_{Q^*}=(1/\tau_{tun})(1-F^*g_{NS}) . \tag{40}$$

Figure 7 shows $\tau_{Q^*}(T)/\tau_{tun}$, $F^*(T)$, and $g_{NS}(T)$ in this limit where only the proximity effect contributes to charge-imbalance relaxation. At low temperatures, F^* and g_{NS} vanish, so $1/\tau_{Q^*}=1/\tau_{tun}$. Near T_c, $F^*\approx 1-\pi\Delta/4k_BT$ and $g_{NS}\approx 1$, so that $1/\tau_{Q^*}$ is proportional to Δ/k_BT, as expected for an inelastic pair breaker:[2,13]

$$1/\tau_{Q^*}\approx(1/\tau_{tun})\pi\Delta/4k_BT \quad (T\approx T_c) . \tag{41}$$

By combining the general result (27)–(29) for $R_j(T)$ with Eq. (40) for $1/\tau_{Q^*}$, we find

$$R_j(T)/R_N=1/(g_{NS}-F^*g_{NS}) . \tag{42}$$

This result is plotted in Fig. 2. It appears to be independent of $1/\tau_{tun}$, but it is not because F^* and g_{NS} depend implicitly on the pair-breaking rate. For a large pair-breaking rate, i.e., $\hbar/2\tau_{tun}$ comparable to k_BT or Δ, pair-breaking effects on the density of states Δ and q will change $R_j(T)/R_N$ significantly from the values shown in Fig. 2.

Now we examine the effect of externally applied supercurrents and magnetic fields. In the presence of these elastic pair-breaking perturbations, the solution for $N_1\delta f_E$ is simply the ratio of the generation rate and the relaxation rate:

$$N_1(E)\delta f_E = \frac{|e|VN_1(E)q}{k_B T \tau_{\rm tun} 4\cosh^2(E/2k_BT)} \times \frac{1}{1/\tau_{\rm tun}+(2/\tau_s)C_{cf}(E)N_1(E)} . \quad (43)$$

Figure 8 shows calculated normalized values of $N_1\delta f_E$ versus energy E, normalized to $\Delta(T/T_c=0.9, 1/\tau_s=0)$, for a SIN junction with $1/\tau_{e\text{-ph}}=0$. As $1/\tau_s$ increases, $N_1\delta f_E$ decreases. The largest depression is at low energies where the coherence factor and density of states are largest. The gap edge also decreases as $1/\tau_s$ increases.

Figure 9 shows how R_j/R_N and $R_{\rm eq}/R_N$ are reduced by a magnetic field for the example junction with $1/\tau_{e\text{-ph}}=0$. A comparison with Fig. 3 for a junction with a finite electron-phonon scattering rate shows that $R_{Q^*}(T)/R_N$ is much larger here, but the low-field inflection point is at about the same field for T near T_c where the inelastic scattering rates are about the same.

A number of effects contribute to the shapes of these curves, as emphasized by the following few figures calculated with parameters appropriate for Sn. As the field is increased, the pair-breaking rate increases, and the charge-imbalance relaxation time τ_{Q^*} decreases, Fig. 10. The order parameter Δ decreases, Fig. 11. The fraction F^* of current to enter the superconductor as quasiparticle charge increases, Fig. 12. At low fields, the dominant effect of the field is to reduce τ_{Q^*}, so that the low-field inflection point in R_j is near the inflection point in τ_{Q^*}. At higher fields, the effects of pair breaking on Δ, F^*, and g_{NS} become dominant, with the ultimate rise in $R_j(T,B_\parallel)/R_N$ near the critical field occurring as $\Delta\to 0$.

Figure 4 plots the normalized pair-breaking rate $\tau_s^{-1}|_{\rm infl}/\tau_{\rm in}^{-1}(T_c)$ at the inflection point in $R_j(B_\parallel)$ versus $B_\parallel$ as a function of T/T_c. The value near T_c is smaller than for the junction including electron-phonon scattering because, in this limit, R_{Q^*} is not quite proportional to τ_{Q^*}. Note the very weak dependence of $\tau_s^{-1}|_{\rm infl}/\tau_{\rm in}^{-1}(T_c)$ on T, reflecting the T-independent rate $1/\tau_{\rm tun}$.

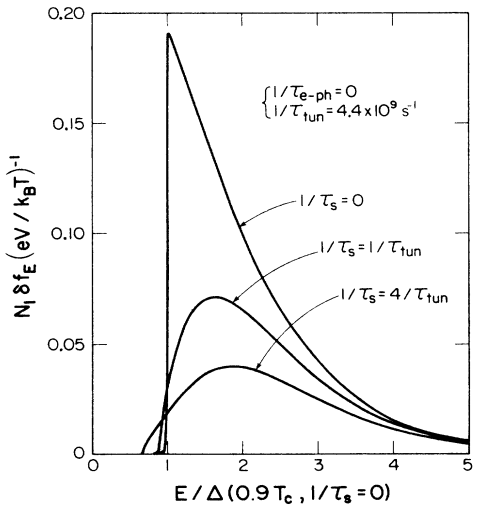

FIG. 8. Normalized nonequilibrium quasiparticle distribution function, $N_1\delta f_E(eV/k_BT)^{-1}$ vs $E/\Delta(0.9T_c, 1/\tau_s=0)$. Curves for different elastic pair-breaking rates $1/\tau_s$ show the reduction in $N_1\delta f_E$ caused by an applied elastic pair breaker. For comparison, the dashed curves in Fig. 6 correspond to the curve labeled $1/\tau_s=4/\tau_{\rm tun}$.

E. Electron-phonon scattering included

With the inclusion of electron-phonon scattering, the equation for δf_E becomes an integral equation. Numeri-

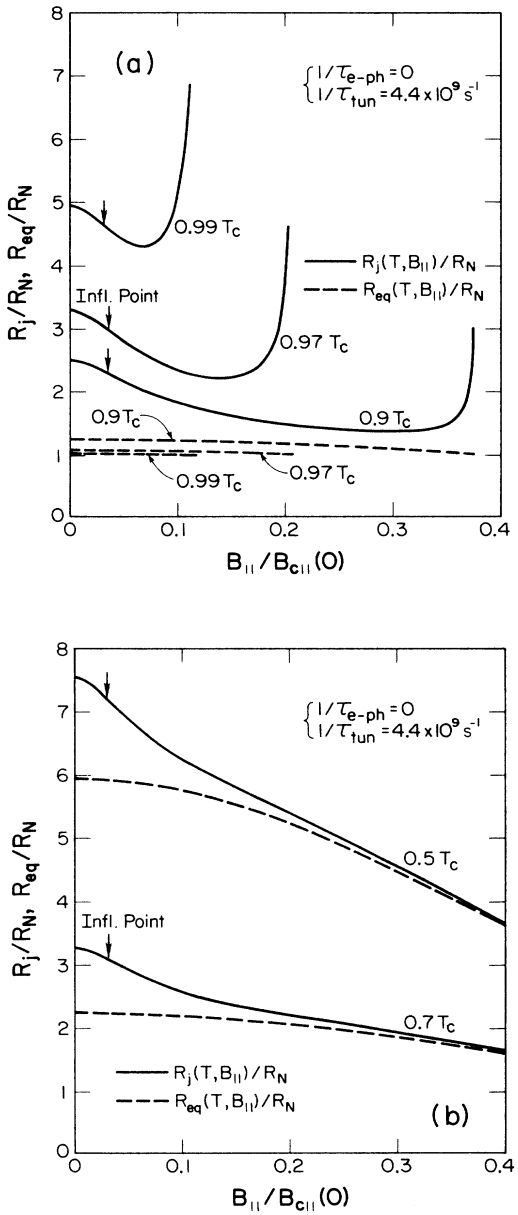

FIG. 9. Calculated resistances R_j/R_N and $R_{\rm eq}/R_N$ vs parallel field $B_\parallel/B_{c\parallel}(0)$ for a hypothetical SIN junction with no electron-phonon scattering in the S film. $R_{\rm eq}/R_N$ is the normalized equilibrium resistance of the junction. Compare with Fig. 3 to see the effect of including electron-phonon scattering.

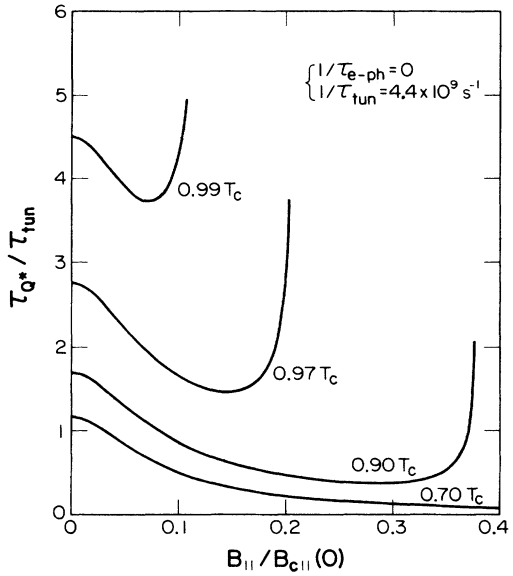

FIG. 10. $\tau_{Q^*}/\tau_{\rm tun}$ vs $B_{\|}/B_{c\|}(0)$ for the SIN junction in which electron-phonon scattering is neglected. Note the similarity between the behavior of $\tau_{Q^*}/\tau_{\rm tun}$ and R_j/R_N (Fig. 9), especially at low fields.

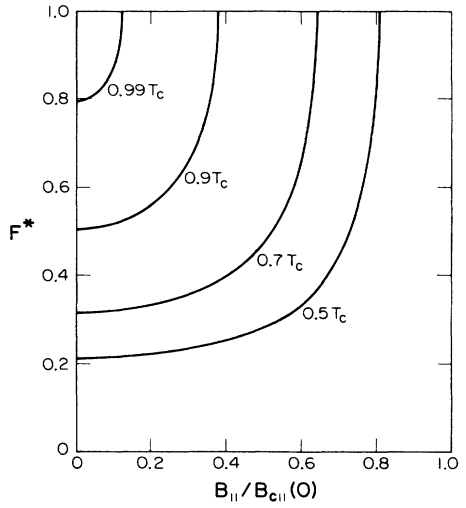

FIG. 12. The fraction F^* of the equilibrium current to enter the S film as quasiparticle charge vs $B_{\|}/B_{c\|}(0)$ for several temperatures.

cal results were presented in Figs. 2–4 above. Here, we wish only to add a discussion of the approximations used to calculate the curves and to illustrate approximately how the effective electron-phonon scattering rate for charge-imbalance relaxation depends on energy and T.

In our calculation of Q^* when electron-phonon scattering is included, we neglect the effects of pair breaking on the coherence factors and density of states in the electron-phonon scattering integral, but include the reduction in Δ. This is valid for small external pair-breaking rates $1/\tau_s \lesssim 1/\tau_{\rm in}$ because then the total rate is also small. For larger external rates, neglecting pair-breaking effects introduces an error in Q^* and hence R_j. However, for large $1/\tau_s$, Q^* is so much reduced that errors in its calculation are relatively unimportant in a calculation of R_j/R_N. Pair-breaking effects on $R_{\rm eq}(T)/R_N$ are important and always included.

We obtain an effective rate $1/\tau_{e\text{-ph}}(E,T)$ by fitting Eq. (43) to values of δf_E calculated with $1/\tau_s=0$. In the fitting, the relaxation rate $\tau_{\rm tun}^{-1}$ in the denominator of Eq. (43) is replaced by

$$\tau_{\rm tun}^{-1}+(\pi\Delta/4k_BT_c)\tau_{e\text{-ph}}^{-1}(E,T)\ .$$

The factor of $\pi\Delta/4k_BT_c$ represents the effective coherence factor for charge-imbalance relaxation due to electron-phonon scattering. Strictly speaking, the coherence factor should always be less than unity, but for this rough analysis, we relax that restriction a little. Figure 13 shows the effective rate as a function of E/k_BT for several temperatures. The effective rate at the lowest energy, $\Delta(T)$, is roughly proportional to T^3. It depends slightly on energy, increasing by about 10% over the relevant energy range from Δ to $\Delta+k_BT$.

Unfortunately, when elastic pair breaking is added this simple model breaks down, and the effective electron-phonon scattering rate determined in this simple way has a complicated energy dependence. Nevertheless, it is pleasing to see the similarity between the effective rate $1/\tau_{e\text{-ph}}(\Delta,T)$ shown in Fig. 13 and the pair-breaking rate at the inflection point in R_j versus $B_{\|}$, shown in Fig. 4.

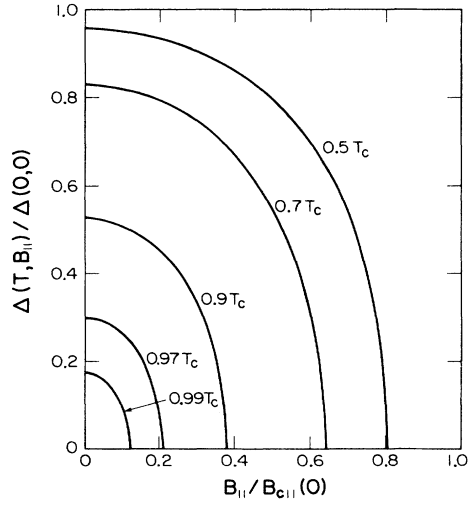

FIG. 11. Normalized order parameter $\Delta(T,B_{\|})$ vs $B_{\|}/B_{c\|}(0)$ for several temperatures.

V. CONCLUSIONS

Our main result is that the dc resistance of low-resistance SIN tunnel junctions contains information about pair-breaking electron-scattering rates, coherence factors, and the density of superconducting electrons in

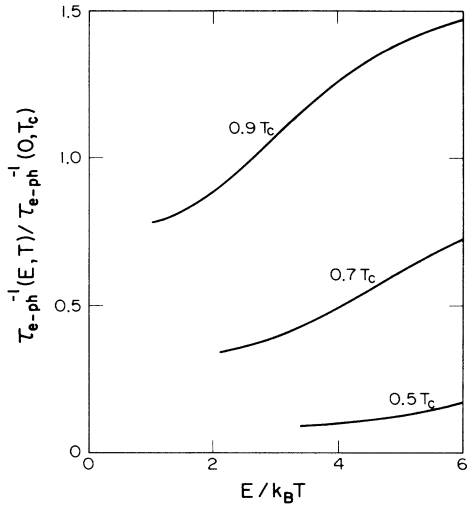

FIG. 13. Normalized effective electron-phonon scattering rate, $\tau_{e\text{-ph}}^{-1}(E,T)/\tau_{e\text{-ph}}^{-1}(0,T_c)$ vs E/k_BT for several temperatures. The value at the minimum energy, $E_{\min}=\Delta(T)$, scales roughly as T^3. The rate depends somewhat on energy, increasing by about 10% over the relevant energy range between Δ and $\Delta+k_BT$.

the S film, and that the information can be obtained through measurements in the presence of supercurrents, either applied directly or induced with a parallel magnetic field. We illustrated in general terms how data might reveal this information with a crude analysis that emphasized the inflection point in R_j versus $B_{\parallel}$ and I_s. With real data, one could do a more precise analysis by doing detailed numerical fits.

There are a number of potential applications for the technique. These include measurements of the pair-breaking rate in weakly disordered superconductors for comparison with the dephasing rate from localization studies,[25] studies of highly disordered superconductors, and measurement of the exchange-scattering rate in superconductors containing magnetic or nearly magnetic dopants. The technique may be especially interesting in studies of novel superconducting materials such as the heavy-fermion superconductors, since it yields information similar to that from other nonequilibrium techniques like NMR and ultrasonic attenuation, but may be easier to apply in some cases since it is a dc measurement.

There is a need for theoretical work in these areas as well. In disordered superconductors, the relative importance of pair breaking due to inelastic electron-electron scattering[26] and elastic scattering in the presence of supercurrent fluctuations[27] is unresolved. In heavily disordered systems, it is unclear how the disorder affects the nature and scattering rates of excitations. Model calculations of the resistance of SIN junctions for the heavy-fermion systems are needed, since it would be very interesting to compare measurements on SIN junctions made with these materials with other nonequilibrium measurements.

ACKNOWLEDGMENTS

This material is based on work supported by the National Science Foundation under Grant Nos. DMR-83-00254 and DMR-85-15370. One of us (T.R.L.) acknowledges support from the Alfred P. Sloan Foundation.

APPENDIX

Various parts of the computer program were checked against analytic or numerical results available in the literature.

The program used to calculate Q^* including electron-phonon scattering and elastic pair breaking was basically the same program used in Refs. 18 and 19. The program accurately reproduces all of the results discussed in those papers. Those results have been reproduced independently.[9]

The program to calculate the order parameter Δ in the presence of pair breaking was based on Ref. 32, and it was checked against plotted results in that paper. The program to calculate the density of superconducting electrons n_s in the dirty limit in the presence of pair breaking was an integral part of the program to calculate Δ. The results were checked by calculating the critical current density $J_c(T)$ from the maximum value of $J_s=n_s(T,\,1/\tau_s)ev_s$ as a function of $1/\tau_s=Dp_s^2/2\hbar^2$, where $p_s=2mv_s$. The results were checked against the usual Ginzburg-Landau result near T_c,[35] and against numerical results in Ref. 36 at lower temperatures.

The program to calculate the density of states $N_1(E)$, the effective quasiparticle charge $q(E)$, and the coherence factor $C_{cf}(E)$ for elastic charge-imbalance relaxation, was based on Ref. 10. The functions $N_1(E)$ and $N_2(E)$ were checked against plotted results in Ref. 9. The functions N_1, N_2, R_1, and R_2 all reduced to the appropriate analytic forms given in Ref. 10 in the limit of zero pair breaking. In addition, calculated values of N_1 for elastic pair breaking only were checked against plotted results in Ref. 32.

[1]M. Tinkham, Phys. Rev. B **6**, 1747 (1972).
[2]A. Schmid and G. Schön, J. Low Temp. Phys. **20**, 207 (1975).
[3]U. Eckern and G. Schön, J. Low Temp. Phys. **32**, 821 (1978).
[4]C. J. Pethick and H. Smith, Ann. Phys. (N.Y.) **119**, 133 (1979).
[5]C. J. Pethick and H. Smith, J. Phys. C **13**, 6313 (1980).
[6]J. J. Chang, Phys. Rev. B **19**, 1420 (1979).
[7]O. Entin-Wohlman and R. Orbach, Phys. Rev. B **21**, 5172 (1980).
[8]A. M. Kadin, L. N. Smith, and W. J. Skocpol, J. Low Temp. Phys. **38**, 497 (1980).
[9]J. Beyer-Nielsen, C. J. Pethick, J. Rammer, and H. Smith, J. Low Temp. Phys. **46**, 565 (1982).

[10]J. Beyer-Nielsen, Ph.D. thesis, H. C. Oersted Institute, 1983 (unpublished).
[11]A. G. Aronov and R. Katilyus, Zh. Eksp. Teor. Fiz. **68**, 2208 (1975) [Sov. Phys.—JETP **41**, 1106 (1976)].
[12]T. R. Lemberger, Phys. Rev. Lett. **52**, 1029 (1984).
[13]T. R. Lemberger, Phys. Rev. B **29**, 4946 (1984).
[14]J. Clarke, Phys. Rev. Lett. **28**, 1363 (1972).
[15]J. Clarke and J. L. Paterson, J. Low Temp. Phys. **15**, 491 (1974).
[16]M. V. Moody and J. L. Paterson, J. Low Temp. Phys. **34**, 83 (1979).
[17]C. C. Chi and J. Clarke, Phys. Rev. B **19**, 4495 (1979); **21**, 333 (1980).
[18]T. R. Lemberger and J. Clarke, Phys. Rev. B **23**, 1088 (1981).
[19]T. R. Lemberger and J. Clarke, Phys. Rev. B **23**, 1100 (1981).
[20]T. R. Lemberger, Phys. Rev. B **24**, 4105 (1981).
[21]T. R. Lemberger and Y. Yen, Phys. Rev. B **29**, 6384 (1984).
[22]Y. Yen and T. R. Lemberger, in *Proceedings of LT17*, edited by U. Eckern, A. Schmid, W. Weber, H. Wühl (North-Holland, Amsterdam, 1984), p. 429.
[23]Y. Yen and T. R. Lemberger (unpublished).
[24]For several reviews and further references, see *Nonequilibrium Superconductivity, Phonons and Kapitza Boundaries,* Proceedings of the NATO Advanced Study Institute, edited by K. E. Gray (Plenum, New York, 1981).
[25]For a recent review, see G. Bergmann, Phys. Rep. **107**, 1 (1984).
[26]W. Eiler, J. Low Temp. Phys. **56**, 481 (1984).
[27]T. R. Lemberger, Physica **107B**, 163 (1981).
[28]S. B. Kaplan, C. C. Chi, D. N. Langenberg, J. J. Chang, S. Jafarey, and D. J. Scalapino, Phys. Rev. B **14**, 4854 (1977).
[29]T. Y. Hsiang and J. Clarke, Phys. Rev. B **21**, 945 (1980).
[30]W. L. McMillan, Phys. Rev. **175**, 537 (1968).
[31]C. Kittel, *Introduction to Solid State Physics,* 5th ed. (Wiley, New York, 1976).
[32]K. Maki, in *Superconductivity,* edited by R. D. Parks (Dekker, New York, 1969), p. 1037.
[33]R. Nicolsky and S. Frota-Pessoa, J. Low Temp. Phys. **46**, 107 (1982).
[34]J. Clarke, U. Eckern, A. Schmid, G. Schön, and M. Tinkham, Phys. Rev. B **20**, 3933 (1979).
[35]See, for example, M. Tinkham, *Introduction to Superconductivity* (McGraw-Hill, New York, 1975), p. 117.
[36]J. Romijn, T. M. Klapwijk, M. J. Renne, and J. E. Mooij, Phys. Rev. B **26**, 3648 (1982).